ExHFT-7
28 June – 03 July 2009, Krakow, Poland

DEVELOPMENT OF MICRO PLASMA ACTUATOR FOR ACTIVE FLOW CONTROL

S. Okochi*, N. Kasagi, Y. Suzuki, S. Ito
Department of Mechanical Engineering, The University of Tokyo, Tokyo 113-8656, Japan

ABSTRACT. We establish the design and fabrication of mm-size plasma actuators through MEMS process. The flow induced by three differently sized actuators fabricated is measured by laser Doppler velocimetry (LDV) in order to clarify these actuators' characteristics. The present experiment first confirms the same dependency of the induced velocity on the imposed voltage as reported in previous work. Then, it is clarified that there exists the optimal frequency to drive a flow unlike previous studies. In the measurement of the flow field, strong suction as well as blowing near the actuator is found in accordance with conventional large plasma actuators. Moreover, distinct suction and blowing in the lateral direction is also identified when reducing the length of actuator. The efficiency of plasma actuator is not changed significantly through miniaturization. These results show that the micro plasma actuator is applicable to various flow controls, particularly, to turbulent flows where small scale structures should be directly manipulated.

Keywords: plasma actuator, miniaturization, MEMS, flow control, turbulence control

INTRODUCTION

Active and flexible flow control has recently attracted much attention due to economical and ecological interests in various industrial applications. For example, efficient flow control systems could modify the laminar-turbulent flow transition in a boundary layer, prevent or induce separation, reduce drag, stabilize or mix air flow in order to avoid undesirable vibration, noise and energy losses [1]. To achieve such flow controls, many actuators have been developed, e.g., mechanical flaps and wall synthetic jets [2, 3]. These actuators have been successfully applied to mixing control in jet, separation control, and so forth. However, they have some drawbacks; generally, they have complicated structures and generate noise, vibration and secondary flow.

In the middle of the 1990s, Roth *et al.* [4] developed a plasma actuator using atmospheric pressure dielectric barrier discharge. Figure 1 shows the configuration of a typical plasma actuator. A plasma actuator (PA, hereafter) consists of two metallic electrodes asymmetrically mounted on both sides of a dielectric plate and lower electrode is covered with dielectric. They demonstrated that a PA drives gas in the area within a few millimeters away from the actuator surface. So far, PAs have been successfully applied to flow separation control or noise reduction. For example, Roth *et al.* [4] have shown the ability of this actuator to modify the properties of a boundary layer over a flat plate, and Göeksel *et al.* [5] have shown lift improvement in stall configuration.

Considering possible advantages such as no moving parts, simple structure and high frequency response, PA is considered promising also for turbulence drag or mixing control. Suppose we consider friction drag reduction in wall turbulence, the momentum transfer is governed by

* Corresponding author: S.Okochi
Phone:+81-3-5841-6419, Fax: +81-3-5800-6999
E-mail address: okouti@thtlab.t.u-tokyo.ac.jp

microscopic coherent structures, whose length and time scales are 10 μm ~ 1 mm and 0.01 ~ 10 ms in practical applications. Therefore, to achieve active and flexible control in such flows, a small PA (1 mm or less) is strongly needed. The most of the PAs reported so far are one with a width of 20 mm and a length of 300 mm. Since the typical length scale of plasma is about a few millimeters, further miniaturization of a PA bellow this length should affect the dynamics of plasma and the resultant performance. We refer to a PA whose electrode width is less than plasma volume (4 mm) as micro PA. Moreover, for the miniaturization of the plasma actuator, to fabricate micro PAs tolerant to high voltage and plasma is a major issue. Therefore, the aim of this paper is: (1) to establish the fabrication process of micro plasma actuator; (2) to clarify the size characteristics of micro and macroscopic plasma actuators; (3) to explore the induced flow velocity and efficiency of micro plasma actuator.

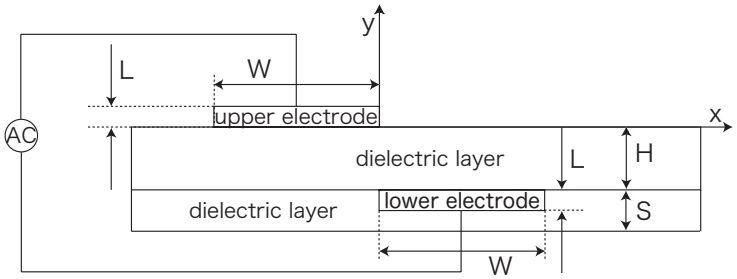

Figure 1. Structure and geometrical parameters of DBD plasma actuator

FABRICATION OF PLASMA ACTUATOR AND EXPERIMENTAL SETUP

Design and fabrication of micro plasma actuator by MEMS

The electrical and mechanical characteristics of a PA depend on various parameters such as electrode width, electrode thickness and dielectric layer thickness. According to Roth *et al.* [4], Forte *et al.* [6] and Hoskinson *et al*. [7], the induced flow is enhanced with decreasing the thicknesses of electrodes and dielectric layer. Based on the knowledge, we designed test actuators are as follows. The electrode width *W* is changed as 1, 4 and 10 mm to investigate the effects of the actuator size on the plasma volume and the induced flow. The electrode thickness *L* is 300 nm, which is the minimum durable thickness through the microelectromechanical system (MEMS) fabrication process we employ. The thickness of a dielectric layer *H* is chosen as 0.525mm, whish is the minimum thickness to avoid dielectric breakdown. The insulate layer thickness *S* is 30 μm to avoid discharge by the lower electrode.

The MEMS fabrication process of micro PA is shown in Fig. 2. The process starts with a 525 μm-thick Pyrex glass wafer. Upper and lower Cr/Au/Cr electrodes are vapour-deposited with a standard lithography process. Then, the lower electrode is covered with Parylene C. Micro PA fabricated by this MEMS process is shown in Fig. 3.

Electric power supply

Figure 4 shows a power supply system used in this experiment. In order to achieve dielectric discharge, the upper electrode is connected to a high voltage amplifier (HEOPT-5B20-L1, ± 5kV) driven by a function generator delivering a sinusoidal waveform. The lower electrode is grounded. A sinusoidal wave voltage with the maximum amplitude up to 5 kV is applied between the electrodes at different frequencies of 0-20 kHz. The voltage and current are monitored by a fast digitizer. The voltage is measured with an internal probe of amplifier, while the current is measured with a Rogowski coil (1kHz-1GHz, 0.1mA-10A).

Velocity measurement

The micro PA is placed flush on the bottom wall surface of the two-dimensional channel, which is about 5 m long and has a test section of 10 × 50 cm^2. A smoke injector is placed at the intake of the channel in order to supply the flow with small oil particles of 1 μm in diameter. The experiment is carried out at low air velocities (Reynolds number based on the channel height and the centerline velocity ~ 1000) in order to easily discriminate the base flow and the flow induced by the micro PA. Although this wind tunnel is designed long enough to reproduce a fully developed turbulence channel flow at the point of measurement, the root-mean-square streamwise velocity fluctuation remains at about 10% of the local mean velocity near the wall region under such a low velocity condition. However, this magnitude of velocity fluctuation is much smaller than the velocity induced by the actuator.

Figure 5 shows the measurement arrangement with a Laser Doppler Velocimeter (LDV) and the coordinate system with its origin being located on the surface just downstream of the center of the upper electrode. The *x*-, *y*- and *z*-axes are defined in the streamwise, wall-normal and spanwise directions, respectively.

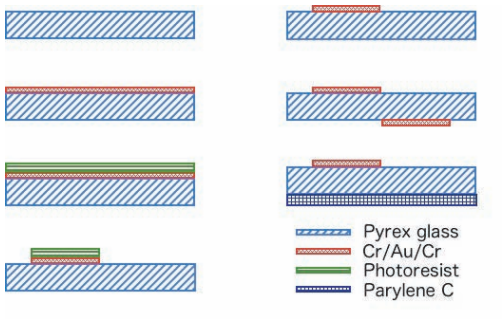

Figure 2. Fabrication process of plasma actuator through MEMS process

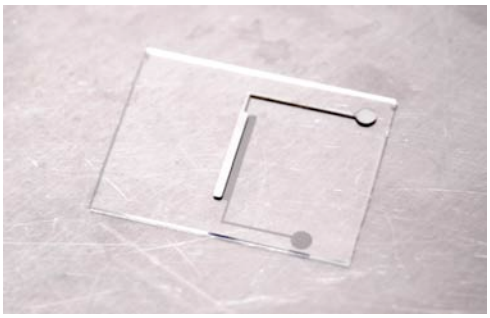

Figure 3. Micro plasma actuator fabricated by MEMS technique (W = 1 mm)

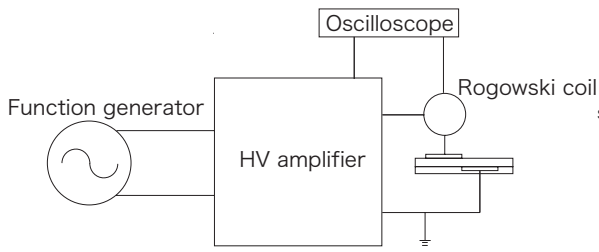

Figure 4. Schematic configuration of the power supply for DBD plasma

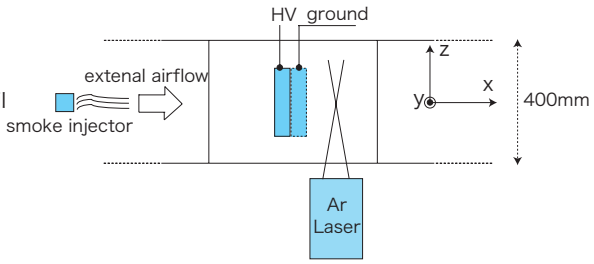

Figure 5. Top view of the LDV system

EXPERIMENTAL RESULTS

Electric discharge and induction of fluid flow

The driving principle of PA is based on the Townsend mechanism, or electron avalanche, which corresponds to the multiplication of some primary electrons in cascade ionization. When a high voltage is applied between two planes, electrons are accelerated towards the anode by the electric field and they ionize the gas by collisions. An avalanche develops because the multiplication of electrons proceeds along their drift from the cathode to the anode. A discharge current is then created.

Figure 6 shows a typical example of the measured voltage and current (W = 1 mm, V_a = 5 kV and F = 10 kHz). It can be seen that the current has two components. One is a sinusoidal wave in

quadrature phase with the voltage. The other is the impulse current due to the dielectric barrier discharge during the positive and negative half-cycles of the voltage waveform. Note that the discharge is asymmetric during the positive and negative cycle. This demonstrated that the discharge is different during the positive and negative cycles as shown in Fig. 6.

Figure 7 presents the instantaneous velocity induced at x = 5 mm, y = 0.5 mm and z = 0 mm by a plasma actuator (V_a = 5 kV, F = 10 kHz, W = 1 mm). The induced flow is fluctuating because the discharge does not behave similarly during the positive and negative cycles. As the barrier discharge is periodic, it seems to generate a pulsating flow. In fact, Forte *et al*. [6] demonstrated that the induced velocity follows the high voltage waveform frequency.

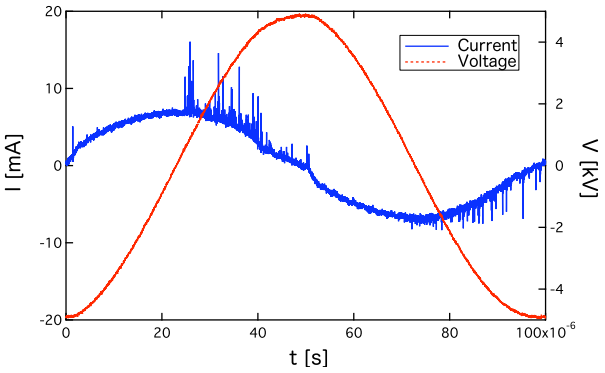

Figure 6. Typical discharge current and voltage waveform

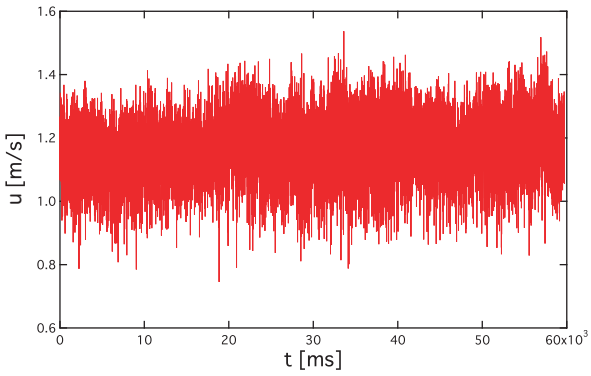

Figure 7. Instantaneous velocity versus time at x = 5 mm and y = 0.5 mm

Time-averaged flow distribution

The velocity field induced by the actuator is measured in the x-y plane with the applied voltage of V_a = 5 kV at the frequency of F = 10 kHz. The time-averaged velocity distributions are shown in Fig. 8. Strong suction is observed between the upper and lower electrodes, and a wall-tangential jet is induced in the vicinity of the wall regardless of the size of plasma actuators. These velocity profiles clearly show the momentum transferred from the plasma to the surrounding air. Specifically, the maximum velocity decreases and the controlled area becomes thicker with increasing streamwise distance x. The maximum induced velocity is enhanced with increasing the actuator size. The peak position of induced velocity in the present study is different from that in the previous research. Forte *et al.* [6] demonstrated that the maximum induced velocity was reached at the end of the plasma, and the induced velocity decreased further downstream. In the present work, in the case of electrode width of 4 and 10 mm, the maximum velocity occurs at the end of the plasma and the height is y = 0.5 mm from the wall. In contrast, in the case of actuator of 1mm width, the maximum velocity is measured at x = 3 mm, not at the end of plasma. This fact is in contrast to the previous results.

Figure 9 shows the flow distribution of the actuator of 1mm in width at different z locations. It is clear that the peak location of induced velocity shifts downstream (x = 3 mm at z = 0 mm, x = 10 mm at z = 3 mm and x = 15 mm at z = 6 mm). Associated with shortening the spanwise length of electrode, it is expected that in the x-z plane where $x < 0$, the induced flow is sucked to the actuator, whereas induced away from it where $x > 0$.

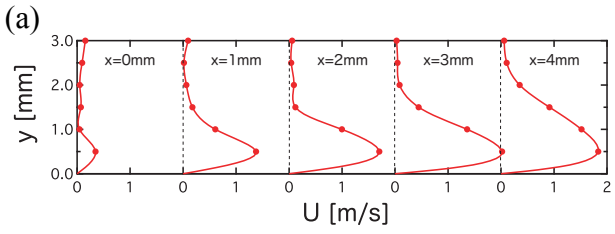

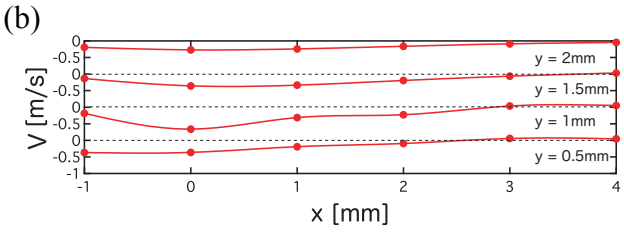

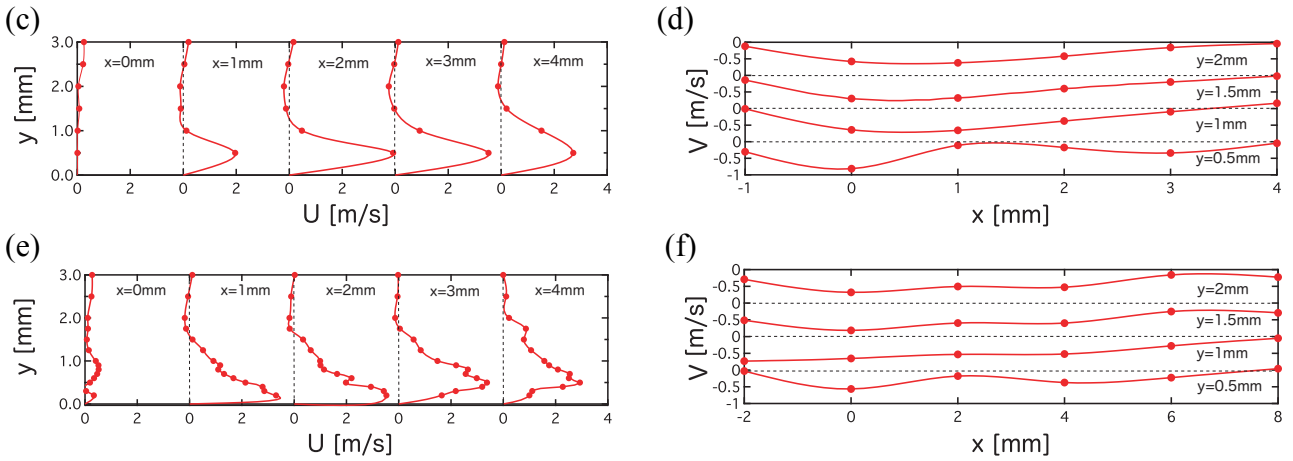

Figure 8. Mean streamwise and wall-normal velocities around the plasma actuator: (a) U with W = 1 mm, (b) V with W = 1mm, (c) U with W = 4 mm, (d) V with W = 4 mm, (e) U with W = 10 mm, (f) V with W = 10 mm

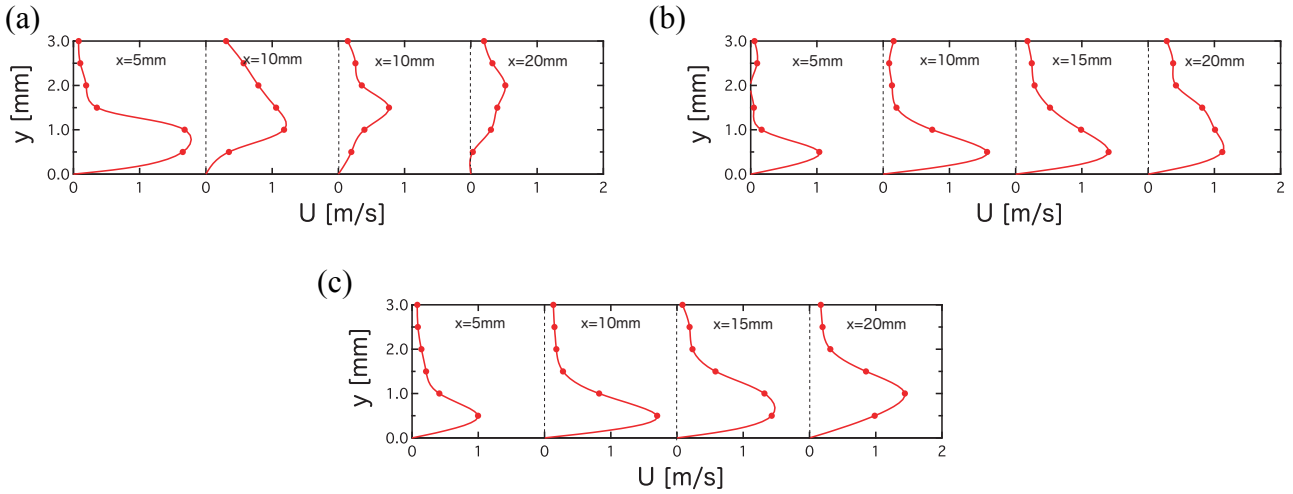

Figure 9. Mean streamwise velocity distributions at different z-planes around the plasma actuator of W = 1 mm: (a) z = 0 mm, (b) z = 3 mm, (c) z = 6 mm

Dependency of induced flow velocity on applied voltage

Figures 10 and 11 respectively show the maximum induced velocity $U_{\max}$, which is measured at the height of y = 0.5 mm, and the electrical power dissipation per unit length P_{elec} at different V_a with F = 5 kHz. The velocity increases monotonously as the applied voltage is increased, because a higher voltage enhances discharge and makes ions undergo stronger Colombian forces. Moreau *et al.* [8] obtained the following empirical equation: $U_{\max} = 0.000166 \times V_a^{3.5}$. In the present work, the relationship between $U_{\max}$ and V_a is approximated as: $U_{max} \propto V_a^{1.8}$, $U_{max} \propto V_a^{1.94}$, and $U_{max} \propto V_a^{2.3}$ for W = 10, 4 and 1 mm, respectively. This difference is due to different discharge modes. It is noted that there is a threshold voltage, at which the discharge mode is changed from glow discharge to filamentary discharge. It is known [6] that the latter filamentary mode of plasma is much less efficient in transferring momentum to neutral gas molecules. However, this threshold voltage is different according to the geometry of PA. Similarly, the electrical power dissipation increases with the applied voltage. The relationship between them is expressed as $P_{elec} \propto V_a^{2.7}$. This result agrees with previous work. For example, Pons [9] and Roth *et al.* [4] demonstrated that $P_{elec} \propto V^n$ with $2 < n < 3$. However, these empirical equations are not based on plasma physics, so that a theoretical approach is needed to establish firm fundamental knowledge.

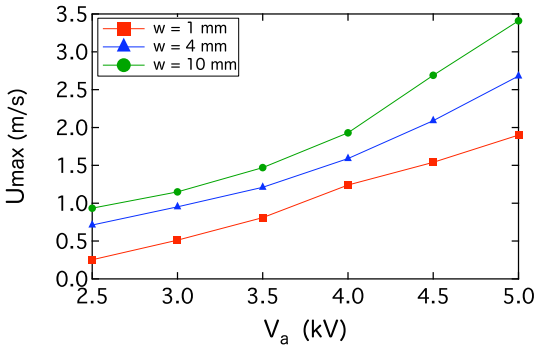

Figure 10. Maximum induced flow velocity versus applied voltage

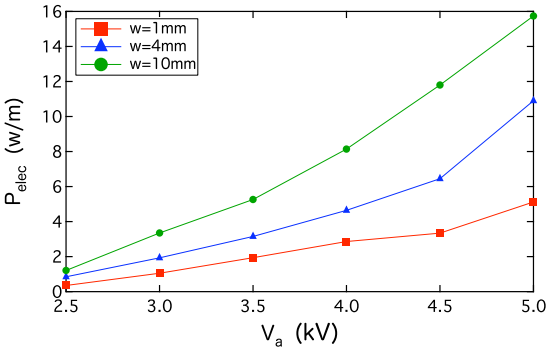

Figure 11. Electrical power dissipation per unit length versus applied voltage

Dependency of induced flow velocity on applied frequency

The maximum induced velocity and the electrical power dissipation per unit length at different frequencies with V_a = 5 kV are shown in Figs. 12 and 13, respectively. It is evident that the optimal frequency to achieve the highest maximum velocity exists and it increases with decreasing the size of the actuator. For example, the optimal frequency is 16 kHz when W = 1 mm, while 12 and 10 kHz for W = 4 and 10 mm, respectively. This fact is in contrast to the previous results, where the induced velocity was monotonically increased with the frequency [6]. The possible reason for this is that, as the frequency is increased, the mean transferred charge increases inducing more collisions between ions and gas and enhancing the induced velocity. However, when the discharge frequency exceeds the ion trapping frequency, the electron avalanche does not grow enough.

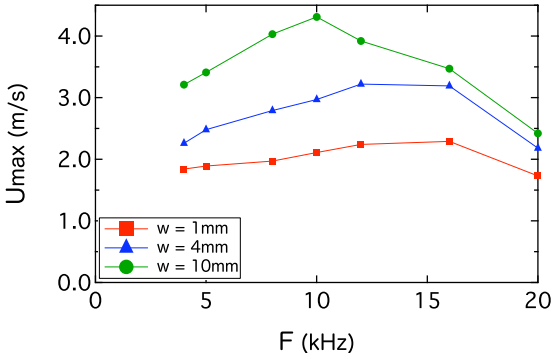

Figure 12. Maximum induced flow velocity versus frequency

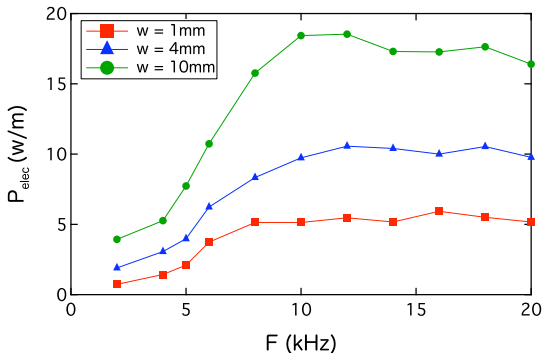

Figure 13. Electrical power dissipation per unit length versus frequency

Efficiency of micro plasma actuator

For a given two-dimensional parallel velocity profile, the corresponding mechanical power delivered to the air can be estimated from the following equation (Moreau [8]):

$$P_{mech} = \int_0^\infty \frac{1}{2} \rho v(y)^3 l dy \ , \tag{1}$$

where ρ is the air density and l is the electrode length. The electrical power dissipation is expressed by the following equation:

$$P_{elec} = \frac{1}{T} \int_0^T V \times I \ dt \tag{2}$$

Then, the mechanical efficiency of a PA is given as:

$$\eta = P_{mech} / P_{elec} \tag{3}$$

The efficiency of micro PA is shown in Fig. 15. It shows that, as the imposed voltage is increased, the electro–mechanical efficiency of a smaller PA reaches its seemingly saturated value faster. Moreover, the efficiency obtained in the present work is much higher than that reported in the previous work. For example, Forte *et al.* [6] demonstrated that the efficiency of PA remains at about 0.03 % as seen in Fig. 15. Figure 16 shows the comparison of maximum induced velocity between conventional and micro PAs. It is clear that the inception voltage of the present micro PA is 2.5 kV and much lower than that reported in previous work. For example, in Forte *et al.* [6], the inception voltage was 8 kV. This is because the employment of a thinner dielectric layer enhances the electric field. Therefore, the efficiency of PA can be even more improved by optimizing design parameters.

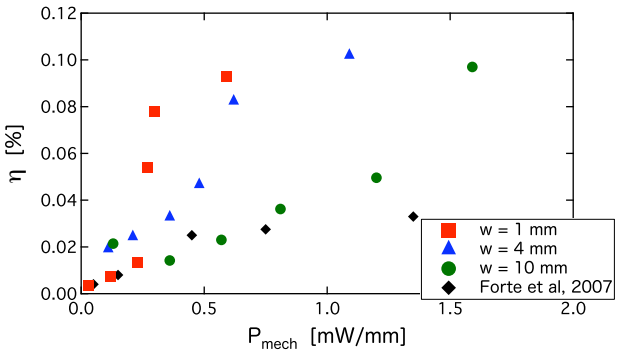

Figure 15. Comparison of the efficiency between conventional and micro plasma actuators

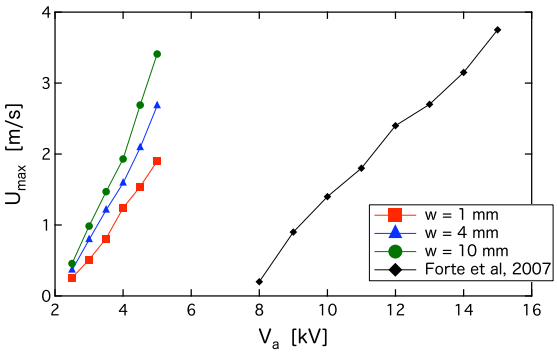

Figure 16. Comparison of the maximum induced velocity between conventional and micro plasma actuators actuator

CONCLUSIONS

In the present work, we proposed and established the MEMS fabrication of micro plasma actuators, of which electrode width is less than the plasma volume size. Then, we experimentally clarified the induced flow characteristics and also the efficiency of the micro plasma actuator. The major findings are summarized as follows:

(1) From the LDV measurement of the flow field, it is confirmed that strong suction and blowing are induced around the plasma actuator regardless of the actuator size tested, i.e., W = 1, 4, and 10 mm. In addition, the induced flow field is essentially three-dimensional because the appreciable spanwise velocity component is also induced, particularly around a smaller plasma actuator.
(2) It is found that the design parameters of plasma actuator affect the discharge and thus the induced velocity considerably. The maximum induced velocity increases with increasing the grounded electrode width and applied voltage, while the optimal driving frequency exists depending upon the size of actuator.
(3) The maximum electro-mechanical efficiency of plasma actuator has weak dependency on the size of the plasma actuator. However, thinning the dielectric layer leads to a higher efficiency.

ACKNOWLEDGEMENTS

We thank Dr. Y. Hasegawa, Messrs. Y. Hamana and D. Ko in the Department of Mechanical Engineering, the University of Tokyo for their discussions and technical supports. The present work was supported through Grant-in-Aid for Scientific Research (A) (No. 20246036) by MEXT, Japan.

REFERENCE

1. Gad-El-Hak M 2000 *Flow Control* (Cambridge: Cambridge university Press)
2. David A and Michael A., Active control of a free jet using a synthetic jet, *International Journal of Heat and Fluid Flow* 29 (2008) 967-984
3. Angele K, Kurimoto N, Suzuki Y and Kasagi N., Evolution of the streamwise vortices in a coaxial jet controlled with micro flap actuators, *Journal of Turbulence*, Volume 7, No. 73, 2006
4. Roth J R and Dai X., Optimization of the Aerodynamic Plasma Actuator as an Electrohydrodynamic (EHD) Electrical Device, *44th AIAA Aerospace Sciences Meeting and Exhibit*, 9 – 12 January 2006
5. B. Göksel, I. Rechenberg, S. Grundmann, C. Tropea, Plasma Actuators for Active Flow Control. DGLR-2005-210, Deutscher Luft- und Raumfahrtkongress, Friedrichshafen, Germany.
6. Forte M *et al.*, Optimization of a dielectric barrier discharge actuator by stationary and non-stationary measurements of the induced flow velocity: application to air flow control, *Experimental Fluids* 43: 917-928, 2007
7. Hoskinson A R, Hershkowitz N and Ashpis D E, Force measurements of single and double barrier DBD plasma actuators in quiescent air, *Journal of Physics D: Applied Physics*. 41 (2008)
8. Moreau E., Airflow control by non-thermal plasma actuators, *Journal of Physics D: Applied Physics*. 40 (2007) 605-636
9. Pons J, Moreau E and Touchard G., Asymmetric surface dielectric barier discharge in air at atmospheric pressure: electrical properties and induced airflow characteristics, *Journal of Physics D: Applied Physics*. 38 (2005) 3635-3642